Psychoacoustic analysis of contra-rotating propeller noise for Unmanned Aerial Vehicles

Antonio J. Torija,[1] [a] Paruchuri Chaitanya,[2,] and Zhengguang Li[3]

[1] *Acoustics Research Centre, University of Salford, Manchester, M5 4WT, United Kingdom*

[2] *Institute of Sound and Vibration Research, University of Southampton, Southampton, SO17 1BJ, United Kingdom*

[3] *Department of Architecture, Zhejiang University of Science and Technology, Hangzhou, 310023, P.R. China*

Unmanned aerial vehicle (UAV) technologies are rapidly advancing due to the unlimited number of applications from parcel delivery to people transportation. As the UAV market expands, community noise impact will become a significant problem for public acceptance. Compact drone architectures based on contra-rotating propellers bring significant benefits in terms of aerodynamic performance and redundancy to ensure vehicle control in case of component failure. However, contra-rotating propellers are severely noisy if not designed appropriately. In the framework of a perception-influenced design approach, this paper investigates the optimal rotor spacing distance configuration to minimise noise annoyance. On the basis of a series of psychoacoustic metrics (i.e. loudness, fluctuation strength, roughness, sharpness and tonality) and psychoacoustic annoyance models, the optimal rotor axial separation distance (expressed as a function of propeller blade diameter) is at a range of 0.2 to 0.4. This paper also discusses the performance of currently available psychoacoustic models to predict propeller noise annoyance, and defines further work to develop a psychoacoustic annoyance model optimised for rotating systems.

[a] A.J.TorijaMartinez@salford.ac.uk

I. INTRODUCTION

New aviation markets, such as Urban Air Mobility (UAM) operations for passengers and drone operations for goods' deliveries and blue light services, are estimated to have a global potential of between $132 and $227 billion over the next 20 years (ATI, 2019). As the drone delivery market intensifies over the coming years, the payload requirement is predicted to increase by a factor of 50 to 100, leading to further problems with their public acceptance; with noise becoming a primary focus. This increase in payload requirements can only be achieved with compact drone architectures such as co-axial or overlapping propellers. The use of contra-rotating propellers in Unmanned Aerial Vehicles (UAVs) has the benefit of increasing aerodynamic performance (Stract et al., 1981), reducing the UAV's plan size and adding redundancy in case of component failure (McKay et al., 2019).

However, the small tip-to-tip spacing between contra-rotating propellers results in a significant source of noise due to blade interaction effects (Tinney and Sirohi, 2018; Alexander et al., 2019). Extensive laboratory testing has found that in the frequency spectra of multi-rotor UAV there are significant sound levels at higher harmonics of the blade passage frequency, which seems to be caused by interaction noise from disturbed inflow due to other rotor blades or the fuselage (Magliozzi, 1991; Cabell et al., 2016; Torija et al., 2019). In an experimental investigation of static multi-rotor contra-rotating UAV propellers, McKay et al. (2019) observed that potential field interaction tones are about 20 dB higher than rotor alone tones at typical ground observer locations with a hovering UAV. This suggests that proper design of multi-rotor contra-rotating UAV propellers to minimise interaction between rotors can lead to significant reductions in noise emission.

The noise sources on a co-axial propeller system can be categorized into either rotor self-noise or interaction noise. Rotor self-noise is principally composed of tonal components and has

contributions due to the steady loading and aerofoil thickness, while the broadband component is relatively weak (Marte and Kurtz, 1970). An interaction source is generated when the spiraling wake and tip vortex from the upper propeller interacts with the lower propeller. At sufficiently small rotor separation distances, an additional interaction noise source is present arising from the interaction of the potential near field of each propeller with the other (Heff, 1990). A more recent study by Chaitanya et al. (2020) performed a detailed investigation on the sensitivity of the aerodynamic and aeroacoustic performance to the axial separation distance between a counter-rotating propeller configuration. An optimum separation distance to diameter ratio for maximum efficiency and minimum radiated noise was found to be at 0.25 based on overall sound power level. The reason behind this optimum is attributed to the balance between potential field interactions and tip-vortex interactions radiated from the contra-rotating configuration. The current paper extends their work to perform psychoacoustic optimization of contra-rotating propellers.

Anghinolfi et al. (2016) carried out a psychoacoustic optimization of blade spacing in subsonic, open, or nearly open axial-flow rotors. This optimization focused only on tonal noise and the objective function was based on the Tone-to-Noise Ratio (TNR) metric. They found optimal blade spacing for different numbers of blade rotors as a function of TNR and level of the highest tonal peak. However, these results do not have direct relation to loudness or other psychoacoustic features.

The perception-influenced design approach (Rizzi, 2016) aims to incorporate human response into the process of creating low-noise aircraft. Metrics that correlate well with human response to noise can potentially be incorporated into the aircraft design cycle to effectively reduce community noise impact (Krishnamurthy et al., 2018). Current noise certification metrics do not necessarily reflect the characteristics of noise signatures of unconventional aircraft designs (Rizzi, 2016; Christian and Cabell, 2017; Torija et al., 2019), and therefore may not be able to predict human

response. Torija et al. (2019) found that the Effective Perceived Noise Level (EPNL) is unable to account for the perceptual effect of series of complex tones spaced evenly across the frequency spectrum with relatively even sound levels, which is typical of multi-rotor vehicles (Cabell et al., 2016; Torija et al., 2019). Other metrics, such as the Sound Exposure Level (SEL), do not account for the effects of tonal noise, which is a major contributor towards the perceived annoyance due to aircraft noise (Angerer et al., 1991; Berckmans et al., 2008; More, 2011; White et al., 2017). Therefore, the use of current noise certification metrics for aircraft design might lead to suboptimal solutions.

Psychoacoustic metrics have been widely applied to improve the sound quality of different consumer products, especially in the automotive industry (Lyon, 2003). Psychoacoustic metrics, such as loudness, sharpness, tonality, roughness and fluctuation strength, are good indicators of how the human auditory system reacts to different features of acoustic stimuli (Zwicker and Fastl, 1999). Loudness measures the sensation of sound intensity. Sharpness and tonality describe the perceptual effects of spectral imbalance of the sound towards the high frequency region, and the presence of spectral irregularities or tones respectively. Fluctuation strength and roughness describe how slow and rapid fluctuations, respectively, of the sound level are perceived. The psychoacoustic metrics sharpness, tonality and fluctuation strength have been suggested as good indicators of rotorcraft noise annoyance (Krishnamurthy et al., 2018; Boucher et al., 2020). Investigating the performance of different psychoacoustic metrics to account for the perception of different aspects of aircraft noise, Barbot et al. (2008) found fluctuation strength as a good indicator of perceptual effects of turbulence and sharpness as a good indicator of the perceptual effects of high frequency noise. Torija et al. (2019) found that Aures/Terhardt tonality (Aures, 1985b) improves on the EPNL Tone Correction in terms of accounting for the presence of complex tones in aircraft noise.

72 Perception of mechanical sounds is a complex process due to the amount of noise features
73 involved (e.g. tonal components, amplitude modulated sounds, etc.). To address this issue, Zwicker
74 and Fastl (1999) proposed a model for combining several psychoacoustic metrics into one model to
75 quantify annoyance (hereinafter called Zwicker's model for short). Using the Zwicker's
76 psychoacoustic annoyance (PA) model, relative annoyance degrees of different noise samples can be
77 estimated from measures of loudness, sharpness, fluctuation strength and roughness. However,
78 Zwicker's PA model does not include a factor accounting for the influence of the tonality on noise
79 annoyance. To improve accuracy in the estimation of relative annoyance degrees caused by several
80 types of tonal/atonal noises, Di et al. (2016) carried out an update of Zwicker's PA model aiming at
81 tonal noises. More (2011) developed a modified version of Zwicker's PA model based on the results
82 of seven psychoacoustic tests for several aircraft sounds with varying psychoacoustic parameters.
83 The modified PA model developed by More, which includes a term based on Aures/Terhardt
84 tonality and loudness to account for the perceptual effect of tonal noise, was found able to
85 accurately predict aircraft noise annoyance.
86 The aim of this paper is to perform a psychoacoustic analysis of a single static contra-rotating
87 propeller mounted in an anechoic chamber. A set of psychoacoustic metrics are calculated for a
88 series of far-field microphone measurements with different separation distance between the contra-
89 rotating propellers. The contribution of each noise source component on the co-axial propeller
90 under study is evaluated from a perceptual standpoint, using relevant psychoacoustic metrics.
91 Working towards the development of a framework for the psychoacoustic optimisation of novel
92 aerial vehicles, this paper investigates the optimal distance between contra-rotating propellers to
93 minimise psychoacoustic impact. The performance of PA models to predict noise annoyance for
94 propeller systems is evaluated and discussed. The main assumption in this paper is that PA models

optimized for propeller noise annoyance can be used to inform propeller design for lower psychoacoustic impact.

This paper is structured as follows: Section II describes the experimental setup for acoustic measurements and the metrics for psychoacoustic analysis; Section III presents and discusses the experimental results and are followed by the main conclusions of this work in section IV.

II. EXPERIMENTAL AND PSYCHOACOUSTIC METHODS

A. Experimental set-up and procedure

The overlapping rotor test rig designed and manufactured at the University of Southampton consisted of two FOXTECH W61-35 brushless DC (BLDC) (16 poles) 700W motors mounted on a carbon fibre beam as shown in Fig. 1. A commercially available T-Motor 16 inch 5.4 inch rotor was used for this overlapping rotor propulsion system analysis. Two Hyperion HP-EM2-TACHBL sensors were used to measure the precise Rotations Per Minute (RPM). Two Maytech 40A-OPTO speed controllers were used to accurately control the BLDC motors. The overlapping rig allowed manipulation of the propulsion system in both rotor horizontal separation distance d/D (with D as the rotor diameter) and rotor axial separation distance z/D. z/D rotor separation was achieved by a custom linear actuator traversing the upper rotor. All of the tests for this study were achieved when the lower rotor plane was at least three rotor diameters away from the ground with anechoic wedges beneath. The selected lead screw and stepper motor configuration allows for z/D variations varying of 0.05 to 1. Sixteen z/D positions were tested: 0.05, 0.075, 0.1, 0.125, 0.15, 0.175, 0.2, 0.25, 0.3, 0.35, 0.4, 0.45, 0.5, 0.6, 0.8 and 1. The combined thrust of the dual-rotor propulsion system is varied from 2 to 20N in steps of 2N. Although 10 thrust settings were measured, the results shown in this paper refer to a thrust of 10 N (varying thrusts lead to changes in magnitudes, but do not alter the trends shown below). A detailed description of the rig is presented by Brazinskas (2019).

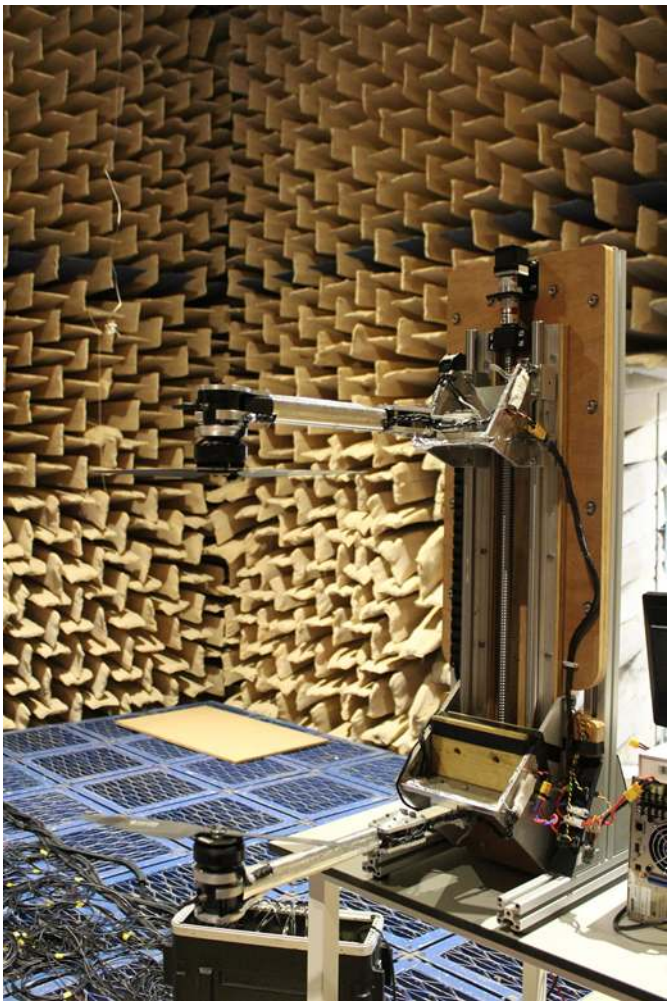

FIG. 1. (Color online). Photograph of overlapping propeller rig within the anechoic chamber of the Institute of Sound and Vibration Research at the University of Southampton.

B. Far-field noise measurements

The overlapping far-field noise measurements were carried out at the Institute of Sound and Vibration Research's open-jet wind tunnel facility. The overlapping rotor test rig was located within an anechoic chamber, of dimension 8 m × 8 m × 8 m as shown in Fig. 1. The walls, acoustically treated with glass wool wedges, allow a cut-off frequency of 80 Hz.

Far-field noise measurements were made using 10, ½ in. condenser microphones (B&K type 4189) located at a constant radial distance of 2.5 m from the centre of the propellers. These microphones were placed at emission angles of between 12 and 102 degrees measured relative to the

129 rotor axis. Measurements were carried out for 10 s duration at a sampling frequency of 50 kHz, and
130 the noise spectra was calculated with a window size of 1024 data points corresponding to a
131 frequency resolution of 48.83 Hz and a Bandwidth-Time (BT) product of about 500, which is
132 sufficient to ensure negligible variance in the spectral estimated at this frequency resolution. Please
133 note that the data analysed in this paper is same as the data presented in Chaitanya et al. (2020).

134 **C. Psychoacoustic data analysis**

135 Unlike physical quantities (e.g. sound pressure level), psychoacoustic metrics provide a linear
136 representation of human hearing perception (HEAD Acoustics, 2018). Psychoacoustic metrics
137 have been found to outperform conventional noise metrics (e.g. EPNL or SEL) in predicting noise
138 annoyance of fixed-wing aircraft (Rizzi et al., 2016; Torija et al., 2019). Recently, several authors
139 (Krishnamurthy et al., 2018; Boucher et al., 2020) have explored the potential of psychoacoustic
140 metrics for the modelling of human annoyance to rotorcraft noise, and assessed the performance of
141 each psychoacoustic metric to account for rotorcraft noise annoyance response.

142 The psychoacoustic metrics (including loudness in sone, sharpness in acum, fluctuation strength
143 in vacil, roughness in asper, impulsiveness in IU, and tonality in TU) of all sound samples were
144 calculated with ArtemiS software (HEAD acoustics GmbH). Loudness was calculated according to
145 DIN 45631/A1 (2010), which is based on Zwicker loudness model and includes a modification for
146 time varying signals. The calculation of sharpness was made according to the standard DIN 45692
147 (2009). This sharpness method does not take into account the influence of absolute loudness on the
148 sharpness perception. There are no standard methods for calculating roughness and fluctuation
149 strength. These two metrics were calculated according to the hearing model given by Sottek (1993).
150 Sottek's hearing model simulates the signal processing of human hearing and accounts for its
151 limitations to track fast temporal changes within a critical band (Boucher et al., 2020). Tonality was
152 calculated according to Aures/Terhardt tonality model (Aures, 1985b).

Three PA models were implemented to discuss their performance in assessing propeller noise annoyance. The Zwicker PA model, accounting for the relation between annoyance and hearing sensations loudness (*N*), sharpness (*S*), fluctuation strength (*F*) and roughness (*R*) is given by

$$PA = N_5\left(1 + \sqrt{w_S^2 + w_{FR}^2}\right) \quad (1)$$

where

N_5 is the 5th percentile of the loudness (in sone)

$$w_S = \{(S - 1.75)\cdot 0.25\lg(N_5 + 10),\ S > 1.75;\ 0,\ S \le 1.75\} \quad (2)$$

$$W_{FR} = \frac{2.18}{N_5^{0.4}}(0.4F + 0.6R) \quad (3)$$

Note that although non specified by Zwicker in the original form of eq. 1, the 5th percentiles of sharpness, fluctuation strength and roughness metrics were used for calculating PA.

The use of 5th percentiles in psychoacoustic analysis is a standard approach widely accepted in the literature. However, these percentile values are dependent on the recording time and the fluctuation of the psychoacoustic parameter in question. This makes that the 5th percentile values for psychoacoustic metrics cannot be compared without appropriate background information. In this research, there is a steady sound pressure during the 10 s duration of each sound sample analysed. For instance, the 5th percentile and arithmetic mean of the loudness for the rotor spacing z/D = 0.05 at azimuthal angle = 12 degrees is 98.5 and 96.4 sones respectively. Therefore, the findings of this research can be argued to be non-dependent of the statistical parameters used to describe the psychoacoustic magnitudes. Furthermore, to avoid the transient effect of the digital filters (used for the computation of the psychoacoustic metrics evaluated) at the start of the audio

174 signal analysis, the first 0.5 s of the sound sample was ignored in the calculation of the 5th percentile
175 of each psychoacoustic metric.

176 As described above, the Zwicker's PA model does not include a factor for accounting for
177 the perceptual effects of tonal sounds. Di et al. (2016) derived a tonality factor (eq. 5) to develop a
178 PA model able to account for the annoyance response of sounds with strong tonal components.
179 The updated PA model developed by Di et al. (2016) (PA') is given by

180 $$PA' = N_5\left(1 + \sqrt{w_S^2 + w_{FR}^2 + w_T^2}\right) \quad (4)$$

181 where

182 $$w_T = \frac{6.41}{N_5^{0.52}} T \quad (5)$$

183 More (2011) developed a modified version of Zwicker PA model optimised to predict
184 aircraft noise annoyance. The More's PA model (PA_{mod}) is given by

185 $$PA_{mod} = N_5\left(1 + \sqrt{\gamma_0 + \gamma_1 w_S^2 + \gamma_2 w_{FR}^2 + \gamma_3 w_T^2}\right) \quad (6)$$

186 where

187 $$w_T^2 = [(1 - e^{-\gamma_4 N_5})^2 \cdot (1 - e^{-\gamma_5 T})^2] \quad (7)$$

188 The estimates for the More's PA model were optimised for aircraft noise on the basis of a
189 series of psychoacoustic tests. The value of these estimates for eqs. 6 and 7, i.e. $\gamma_0 = -0.16, \gamma_1 =$
190 $11.48, \gamma_2 = 0.84, \gamma_3 = 1.25, \gamma_4 = 0.29$ and $\gamma_5 = 5.49$, show the significant emphasis of the
191 More's PA model on sharpness and tonality. Note that 5th percentile of Aures/Terhardt tonality was
192 used for calculating PA in Di et al.'s and More's models.

None of these PA models account for the impulsiveness of the audio signal. Although there is no agreement in the literature, some authors advise that the prevalence of annoyance due to rotorcraft is influenced by its impulsiveness (Mestre et al., 2017). The impulsiveness (measured in IU) of all sound samples were calculated using the Sottek's hearing model. This psychoacoustic metric accounts for the perception caused by short and sudden changes in sound pressure level (Boucher, et al., 2019). A full description of the calculation of the impulsiveness metrics and its computation in the Sottek's hearing model can be found at Sottek et al. (1995) and Sottek and Genuit (2005) respectively. McMullen (2014) suggested that a combination of different psychoacoustic metrics, including loudness, sharpness, tonality and impulsiveness might provide an accurate assessment of human response to helicopter noise. All this suggests that impulsiveness might need to be considered for developing a PA model for rotorcraft noise.

III. RESULTS AND DISCUSSION

A. Directivity and spectra patterns

Figure 2 shows the 5th percentile of loudness (Fig. 2C) and sharpness (Fig. 2D) as a function of azimuthal angle (i.e. emission angles between 12 and 102 degrees measured relative to the rotor axis), for rotor spacings z/D=0.05, 0.2 and 1 and a thrust setting of 10 N. Maximum noise emission (i.e. loudness) is found at the rotor axis. Loudness decreases with azimuthal angle, reaching minimum values at 82-92 degrees (Fig. 2C). The same directivity pattern is observed for all rotor spacing evaluated. This is consistent with Chaitanya et al.'s (2020) previously observed optimum separation distance based on overall sound power level (see Figs. 2A and 2B for equivalent sound pressure level (SPL) and equivalent A-weighted SPL as a function of emission angle). Equivalent SPL, equivalent A-weighted SPL and loudness are lower at rotor spacing z/D=0.2 than at rotor spacings z/D=0.05 and z/D=1.

For all rotor spacings, maximum values of sharpness are observed at azimuthal angles of 82 to 92 degrees (Fig. 2D). Sharpness at rotor spacing z/D=0.2 is higher than sharpness at rotor spacings z/D=0.05 and z/D=1. Directivity patterns of loudness and sharpness metrics seem to be in line with the initial hypothesis that the highest contribution to measured sounds is the noise emission of potential field interaction tones. McKay et al. (2019) found that potential field interaction tones in co-axial propellers have a dipole directivity with a null at 90 degrees. In this research, the dip in the value of equivalent SPL, equivalent A-weighted SPL and loudness at about 82-92 degrees (as shown in Figs. 2A, 2B and 2C) can be attributable to a decline in the noise emission of potential field interaction tones. This slight shift in the dip of noise radiation from 90 degrees to 82 degrees may be due to the contribution of noise sources others than potential field interaction tones, and that in this research the azimuthal angles measured were related to the bottom propeller.

The decline in amplitude of potential field interaction tones at about 82-92 degrees also leads to an important increase in the relative contribution of higher harmonics of the blade passage frequencies (BPFs) and high frequency broadband noise, which is accounted for by an increase of sharpness as shown in Fig. 2D.

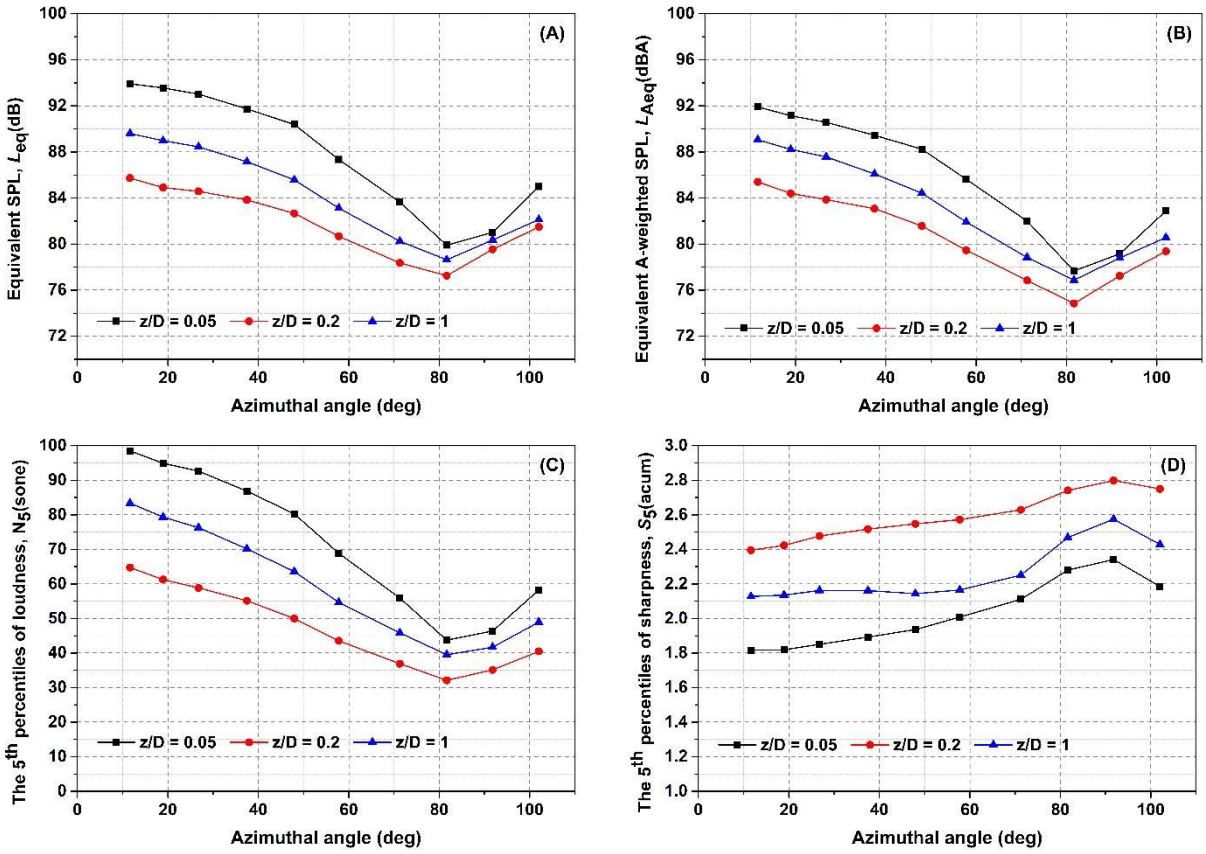

FIG. 2. (Color online). The equivalent SPL (A), equivalent A-weighted SPL (B), and the 5th percentiles of loudness (C) and sharpness (D) as a function of azimuthal angle, for a thrust setting of 10 N and for rotor spacings z/D=0.05, 0.2 and 1.

To continue with the investigation of the individual noise sources in the contra-rotating propeller under study, a narrow band frequency analysis was conducted. Figure 3 shows the narrow band frequency spectra for the rotor spacings z/D=0.05, 0.2 and 1 for azimuthal angles 12 deg (Fig. 3A) and 82 deg (Fig. 3B), and a thrust setting of 10 N. These two azimuthal angles allow the comparison between the narrow band frequency spectra for high loudness (i.e. 12 deg) and high sharpness (i.e. 82 deg).

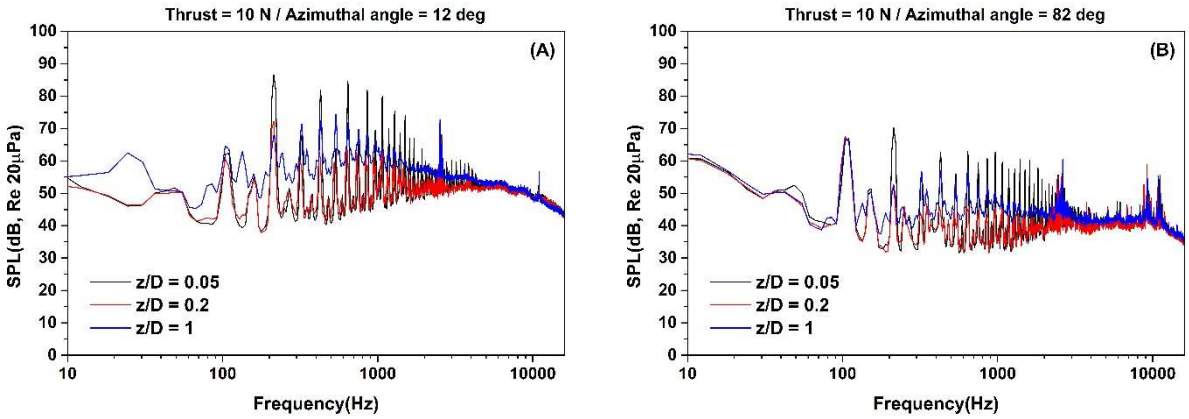

FIG. 3. (Color online). Narrow band frequency spectra for the rotor spacings z/D=0.05, 0.2 and 1 for a thrust setting of 10 N, and for azimuthal angles 12 deg (A) and 82 deg (B).

As shown in Fig. 3, the noise signatures of the contra-rotating propeller measured are dominated by tonal components distributed along the frequency spectrum (between 0.1 and 2 kHz). These tonal components include potential field interaction tones at frequencies that are the summation of rotor BPFs. An analysis carried out by McKay et al. (2019) and Chaitanya et al. (2020) demonstrated that interaction tones are predominantly caused by potential field interactions, and therefore, they decay rapidly with rotor spacing. This decay in amplitude of potential field interaction tones is observed by comparing frequency spectra of rotor spacings z/D=0.05 and 0.2. The decrease in amplitude of potential field interaction tones as rotor spacing increases, leads to a sound signature with higher relative contribution of high frequency components (broadband and tonal components over 2 kHz). As the rotor spacing continues increasing, from z/D=0.05 and 0.2 to z/D=1, the contribution of broadband noise increases. This increase can be attributed to the enhanced interaction between the turbulence generated by the upper propeller tip vortex and the lower propeller as demonstrated by Chaitanya et al. (2020).

At an emission angle of 82 degrees, the amplitude of potential field interaction tones significantly decays (especially for rotor spacing z/D=0.2), due to their dipole directivity (as described above). A decrease of about 20 dB is observed in the amplitude of potential field

interaction tones at 82 degrees compared to the amplitude at 12 degrees (see Fig. 3). For the specific case of rotor spacing z/D=0.05 at 82 degrees, the amplitude of potential field interaction tones is of the same order of magnitude as the amplitude of BPF tones (Fig. 3B). This is due to both the dipole directivity of potential field interaction tones with a null at about 90 degrees and the maximum emission of BPF tones in the plane of the propeller (McKay et al., 2019). At an emission angle of 82 degrees there is a reduction of high frequency broadband noise (compared to 12 degrees), and a series of tonal components of important magnitude are observed in the high frequency region, i.e. 2-12kHz. The precise reason for this behaviour is currently not known and more work is required to understand this phenomenon.

B. Psychoacoustic metrics vs. rotor spacing

To investigate the optimum rotor spacing configuration for the contra-rotating system under study, the value of the different psychoacoustic metrics described above in Section II.C has been calculated. The value of psychoacoustics metrics (5^{th} percentile) as a function of rotor spacing at an azimuthal angle of 12 and 82 degrees is shown in Fig. 4. As described above (Section III.A), at 12 and 82 degrees the contra-rotating system measured has the highest and lowest noise emission respectively.

As the rotor spacing increases, the amplitude of the potential field interaction tones distributed along the mid to high frequency regions decays significantly (see Fig. 3). Consequently, as shown in Fig. 4A, loudness decreases with an increase in rotor spacing, reaching the lowest values at the region z/D=0.2-0.4 at 12 degrees and z/D=0.2-0.3 at 82 degrees. This decay is more significant at 12 degrees (about 30 sone reduction between rotor spacings z/D=0.05 and 0.2) where the emission of potential field interaction tones is maximum, compared to 82 degrees (about 10 sone reduction between rotor spacings z/D=0.05 and 0.2). At small rotor spacings, the decrease in loudness is due to a reduction in the potential field interactions between the two contra-rotating propellers. This

interaction noise is primarily tonal, and hence tonality drops significantly as rotor spacing increases (see Fig. 4B). These results are in line with existing literature (McKay et al., 2019; Chaitanya et al., 2020), where blade spacing optimization has been demonstrated to lead to important reductions in tonal noise (Anghinolfi et al., 2016). Figure 4B shows that, at 12 degrees, there is a significant drop in tonality at a rotor spacing z/D=0.35, to remain almost constant regardless rotor spacing onwards. At 82 degrees, this significant drop in tonality is found at a rotor spacing z/D=0.2 (Fig. 4B). This might be due to the directivity characteristics of potential field interactions, as described in Section III.A. With higher amplitude of potential field interaction tones at emission angles about 0 degrees relative to the rotor axis, a greater rotor spacing is needed at 12 degrees for tonality to drop to minimum values (compared to 82 degrees). At both emission angles, 12 and 82 degrees the same minimum value of tonality is observed at a rotor spacing z/D=0.35 (Fig. 4B).

Fluctuation strength accounts for the low frequency amplitude modulation consequence of the closely spaced potential field interaction tones, as shown in Fig. 3. As rotor spacing increases beyond z/D=0.15-0.2, potential field interactions are reduced (i.e. amplitude of interaction tones decays), and consequently a significant drop in fluctuation strength is observed (Fig. 4C).

With increase in rotor separation distances, interaction noise between rotors increases due to enhanced turbulence-propeller interactions because of unsteadiness in the tip vortex as previously demonstrated by Chaitanya et al. (2020). This added turbulence-propeller interaction noise, which is tonal and broadband in nature (see Fig. 3), causes an increase of loudness after rotor spacing z/D=0.4 (Fig. 4A). Modulated broadband noise reaches higher roughness values than modulated discrete tones, and even unmodulated broadband noise attains considerable roughness values due to random envelope fluctuations (Daniel, 2008). Therefore, the increase in unsteady turbulence-propeller interaction noise as rotors are moved apart might explain the gradual growth of roughness shown in Fig. 4D. At 12 degrees, the highest emission of broadband noise due to unsteady

311 turbulence-propeller interaction noise leads to a higher rate of increase in roughness with rotor
312 spacing (as observed in Fig. 4D).

313 As seen in Fig. 4E, impulsiveness significantly increases as the rotor spacing grows. This is
314 observed for both azimuthal angles of highest and lowest noise emission, although the highest
315 values of impulsiveness are at 12 degrees. As discussed by Krishnamurthy et al. (2018),
316 impulsiveness and roughness metrics are strongly linked to each other. This is observed in this
317 paper by comparing Figs. 4D and 4E. Noise caused by enhanced turbulence-propeller interactions
318 is highly impulsive, and therefore, the added turbulence-propeller interaction noise as the contra-
319 rotating rotors move apart from each other leads to an increase in the impulsiveness metric. This
320 suggests that the impulsiveness metric should be considered, along with roughness, to account for
321 the perceptual response to propeller-turbulence interaction noise in the development of a PA model
322 for rotorcraft noise.

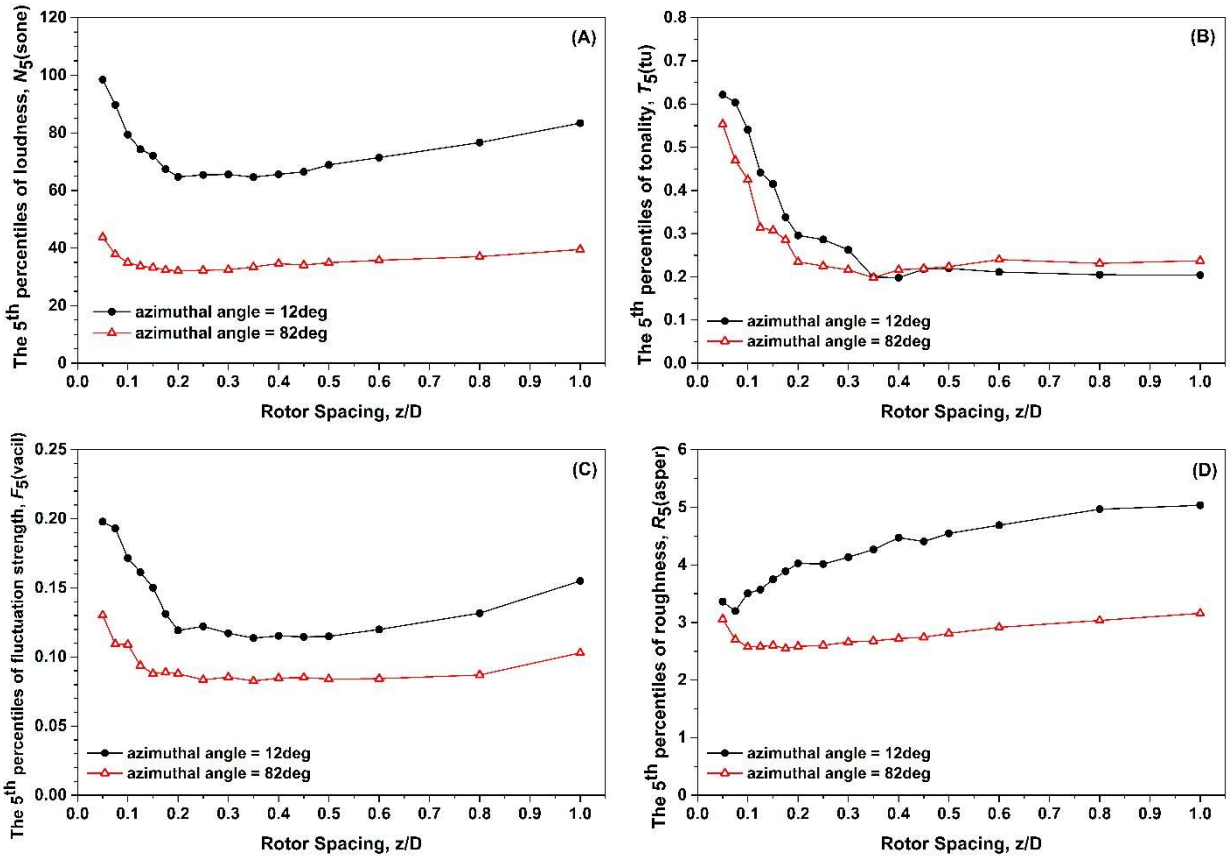

323

324

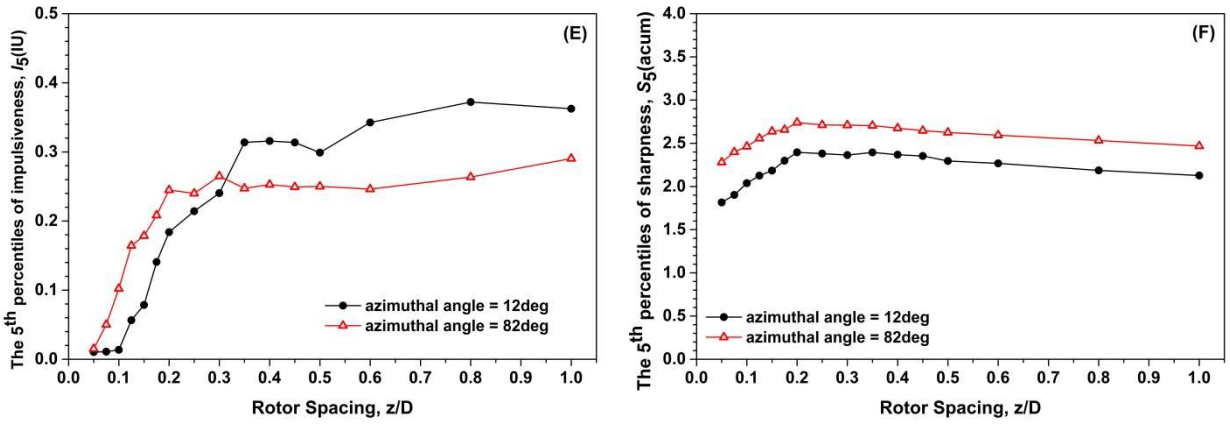

FIG. 4. (Color online). The 5th percentiles of loudness (A), tonality (B), fluctuation strength (C), roughness (D), impulsiveness (E) and sharpness (F) as a function of rotor spacing at azimuthal angle12 deg and 82 deg, for a thrust setting of 10 N.

At rotor spacings in the region z/D=0.2-0.4, the contribution of potential field interaction tones reaches a minimum. This leads to an increase in the relative contribution of high frequency tonal and broadband components (i.e. shaper sounds). Therefore, at rotor spacings z/D=0.2-0.4, the spectral centroid is located at a higher frequency (compared to audio signals of rotor spacings with dominant potential field interaction tones), and therefore higher values of sharpness are observed (Fig. 4F). The same pattern of sharpness as a function of rotor spacing is observed for both 12 and 82 degrees, although sharpness values are higher at 82 degrees due to the lowest emission of potential field interaction tones at these emission angles. Cabell et al. (2016) found important emissions of high frequency tones between 3.5 and 5 kHz for a series of multi-copters driven by brushless DC motors. The noise generated by brushless DC motors is primarily due to both force pulses as the magnets and armature interact and forces caused by phase changes in the motor drive signal (Brackley and Pollock, 2000). Alexander at al. (2019) observed high frequency humps in a series of multi-copters measured at hover configuration. Although the authors state this noise being broadband in nature, its origin is still under investigation.

C. Models for psychoacoustic annoyance

To identify the optimal rotor spacing configuration for the contra-rotating propeller under evaluation, PA as a function of rotor spacing has been calculated according to PA models developed by Zwicker and Fastl (1999), Di et al. (2016) and More (2011). As shown in Fig. 5, as expected from the value of the psychoacoustic metrics analysed in section III.B, the lowest values of PA are found for rotor spacing in the rage of z/D=0.2-0.4 for both 12 and 82 degrees.

At 12 degrees, i.e. the emission angle with the highest amplitude of potential field interaction tones, three main results are observed in Fig. 5A: (i) A significant decay in PA is observed at the optimal rotor spacing area, compared to rotor spacings below z/D=0.2 and above z/D=0.4. (ii) As rotor interaction noise at this rotor spacing is tonal in nature (i.e. potential field interaction tones), Di et al.'s PA model and especially More's PA model (both of which include a tonal factor) lead to lower psychoacoustic annoyance at optimal rotor spacing than Zwicker's PA model. (iii) While Zwicker's and Di et al.'s PA models give the minimum value of psychoacoustic annoyance at rotor spacing z/D=0.2, the lowest psychoacoustic annoyance according to More's PA model is at z/D=0.35. This seems to be due to the higher contribution of the tonal factor in the PA model developed by More (see Fig. 6).

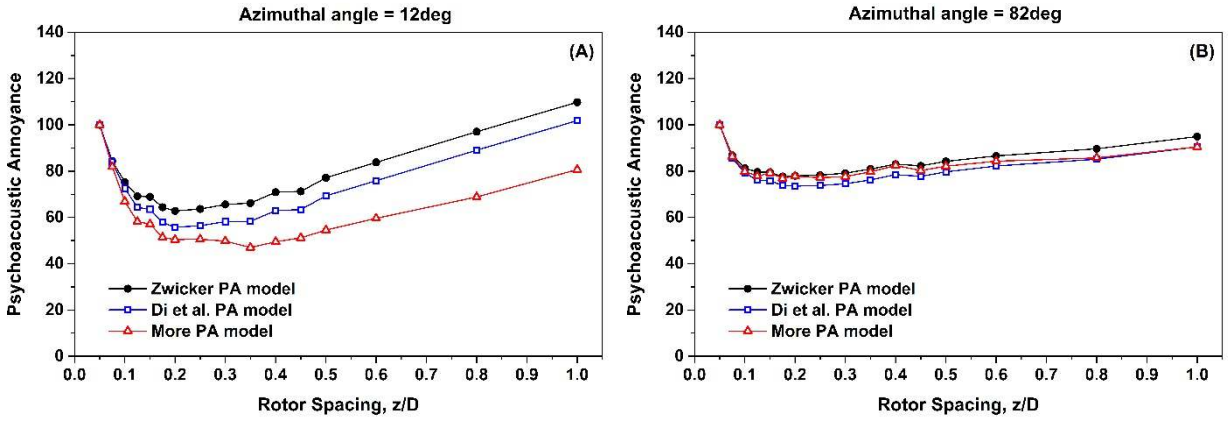

360 FIG. 5. (Color online). Psychoacoustic annoyance (PA) calculated with Zwicker's, Di et al.'s and
361 More's PA models as a function of rotor spacing, for azimuthal angle 12 deg (A) and 82 deg (B) with
362 a thrust setting of 10 N. Normalised to PA = 100 at z/d=0.05.

363 At 82 degrees, i.e. the emission angle with the lowest amplitude of potential field interaction
364 tones, it is observed that the three models implemented give similar values of PA (Fig. 5B). The PA
365 model developed by Di et al. (2016) gives the lowest values of PA among the three models used.
366 The values of PA calculated according to the model developed by More are higher than the values
367 calculated with Di et al.'s PA model for the rotor spacing range z/D=0.15-0.6. This seems to be
368 due to the higher contribution of the sharpness factor in the PA model developed by More (see Fig.
369 4F for sharpness vs. rotor spacing). At this emission angle, the range of variation of PA as a
370 function of rotor spacing is significantly more reduced than at an emission angle of 12 degrees. This
371 finding suggests that a suboptimal rotor spacing between contra-rotating propellers can lead to a
372 significant increase in PA at emission angles in line to the rotor axis. These emission angles are
373 typical for an observer on the ground interacting with a hovering contra-rotating UAV.

374 Zwicker's and Di et al.'s PA models (Zwicker and Fastl, 1999; Di et al., 2016) were derived for a
375 series of mechanical sounds, and More (2011) modified Zwicker's PA model to account for
376 characteristics of fixed-wing aircraft noise. However, none of these PA models have been optimised
377 for propeller noise, and therefore might not be able to account for the complex perceptual
378 interactions between individual noise sources (e.g. tonal components, roughness due to interactions
379 between closely spaced tones, broadband noise in high frequency region due to unsteadiness in the
380 wake, propeller-turbulence interaction noise, etc.). This might lead to important uncertainty in the
381 prediction of PA with current models available. Furthermore, in the three PA models implemented
382 in this work, loudness is included as a first order term, and the other psychoacoustic metrics are just
383 second order factors. For this reason, the calculations of PA with these psychoacoustic models are

384 mainly driven by loudness, and the contribution of other psychoacoustic factors is quite reduced.
385 Sharpness has been found to be an important contributor to aircraft noise annoyance (Torija et al.,
386 2019). Sharpness, tonality and fluctuation strength were found to be important predictors of
387 annoyance for rotorcraft-like sounds (Krishnamurthy et al., 2018; Boucher et al., 2020). Roughness
388 has been found, for instance, an important factor to describing sound quality of electric motors
389 (Mosquera-Sanchez et al., 2014; Ercan, 2019). The relative contribution of psychoacoustic features
390 to annoyance for propeller noise is unknown. A process of listening tests and optimization of
391 coefficients for psychoacoustic terms in PA models, similar to the one carried out by More (2011)
392 for fixed-wing aircraft, is needed for propeller noise.

393 A recent study carried out by Gwak et al. (2020) has investigated the relationship between
394 psychoacoustic metrics and the annoyance reported for a range of hovering UAVs of varying size.
395 The authors found that the annoyance reported for medium and large drones is driven by loudness,
396 sharpness and fluctuation strength; they also found that the annoyance reported for small drones
397 cannot be explained by the three psychoacoustic metrics above, but tonality might play an important
398 role. Based on the β-coefficients of a linear regression model of the annoyance for medium and
399 large drones developed by Gwak et al. (2020, pp. 13), reported annoyance is mainly driven by
400 loudness ($\beta = 0.908$) and sharpness ($\beta = 0.102$) and fluctuation strength ($\beta = 0.268$) are second
401 order contributors. Further, the standardised β-coefficients of the linear regression model indicate
402 that an increase of 0.516 loudness units (i.e. sones) is needed to increase the annoyance in 1 unit[1],
403 while an increase of 9.902 sharpness units (i.e. acum) is needed for an increase in 1 unit of
404 annoyance. Using the results of Gwak et al. (2020), the increase in the contribution of sharpness
405 (relative lo loudness) needed in order for it to dominate the psychoacoustic annoyance calculation is
406 unrealistic. Based on this, one could argue that the optimal rotor spacing, in terms of

[1] Note that annoyance in Gwak et al. (2020) is assessed using a 11-point scale.

psychoacoustic annoyance, suggested in this paper is not subjected to specific models but a more general finding.

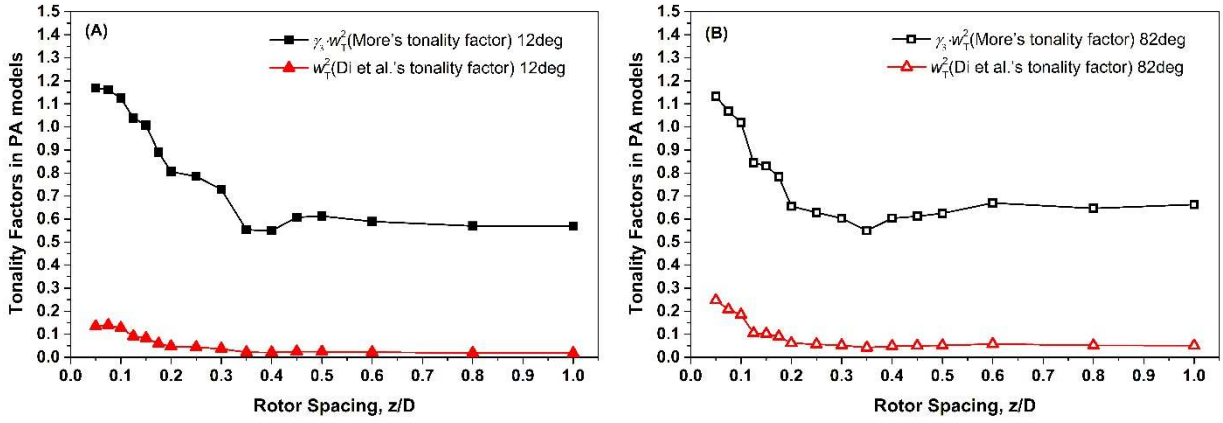

FIG. 6. (Color online). Di et al.'s tonality factor (w_T^2) and More's tonality factor ($\gamma_3 w_T^2$)in PA models as a function of rotor spacing, for azimuthal angle 12 deg (A) and 82 deg (B) with a thrust setting of 10 N.

Although the perceived roughness and impulsiveness might be a factor due to unsteady turbulence-propeller interaction noise, annoyance might be assumed to be primarily driven by perceived tonality in the region of optimal rotor spacing as shown in Figs. 4B and 5 (i.e. sound is eminently tonal in nature in this region due to the contribution of potential field interaction tones). Several studies on a variety of noise sources, such as mechanical ventilation systems (Lee, 2016) and aircraft noise (More and Davies, 2010) have suggested a combination of loudness and tonality factors in multiple linear regression models as an accurate approach to predict annoyance. As seen in Fig. 6, both the tonality factors derived by Di et al. (2016) and More (2011) (accounting for the combined effect of loudness and tonality) suggest the optimal rotor spacing at z/D≥0.35 (note that the minimum value of both tonality factors is at z/D=0.35). Figure 6 shows the Di et al.'s tonality factor squared (eq. 5), and More's tonality factor squared (eq. 7) multiplied by $\gamma_3 = 1.25$ (to account for the total contribution of tonality in More's PA model). This figure also shows that More's

425 tonality factor emphasises more the contribution of tonality in the PA model than Di et al.'s. The
426 value of both tonality factors as a function of rotor spacing demonstrates that More's factor is more
427 sensitive to variations in tonality, and therefore would lead to higher variation in PA for the same
428 changes in tonality.

429 Future work for the development of PA models for propellers, and especially contra-rotating
430 multiple blade propellers, will need to focus on psychoacoustic features such as perceived
431 impulsiveness caused by propeller-turbulence interaction, and perceived roughness and perceived
432 tonality of multiple tone complexes. Perceived roughness of superpositioned multiple pure tones
433 (see Fig. 3) differs from perceived roughness of amplitude modulated tones, even with similar
434 modulation strengths (Terhardt, 1974; Aures, 1985a). Perakis et al. (2013) found that the modulation
435 index of an amplitude modulated tone must be lowered by 2/3 to be perceived as equally rough as a
436 pair of superpositioned tones. This perceptual phenomenon should be taken into account when
437 deriving a fluctuation strength/roughness function accounting for the perceptual interaction effect
438 of closely spaced multiple tones. The perceived tonal strength of mechanical sounds containing
439 series of harmonic or inharmonic complex tones can adversely influence the perception of these
440 sounds (Lee et al., 2005). The prediction of annoyance from sounds containing multiple tone
441 complexes requires not only accounting for the tonality of the most prevailing tone and signal
442 loudness, but also the frequencies and the structure of the other tones in the noise signal (Lee and
443 Wang, 2020). Aures/Terhardt tonality model (Aures, 1985b) accounts for the presence of complex
444 tones. However, Lee at al. (2005) found that Aures/Terhardt tonality model overestimates
445 perceived tonality of complex tones. These authors modified Aures/Terhardt tonality with a factor
446 accounting for the differences in tonality perception between harmonic complexes and single tones,
447 and concluded that the perceived tonality of multiple tone complexes is a function of the pitch
448 strength of the harmonic components. Therefore, pitch perception models, such as Terhardt's

449 virtual pitch model (Terhardt et al., 1982a;b) should be taken into account when deriving a function
450 accounting for the perceived tonality of complex tones in propeller noise.

451 IV. CONCLUSION

452 This paper presents the results of a psychoacoustic analysis carried out to investigate the optimal
453 distance between contra-rotating propellers to minimise noise annoyance. On the basis of
454 psychoacoustic annoyance, calculated with models available in the literature, it can be concluded that
455 the optimal rotor axial separation distance for the contra-rotating propellers under study is at a range
456 of z/D=0.2-0.4, instead of previously observed z/D=0.25 by Chaitanya et al. (2020) on the basis of
457 overall sound power level. Similar optimal rotor spacing is found for azimuthal angles of maximum
458 and minimum emission of potential field interaction tones, which are the highest contributors to the
459 contra-rotating propellers sounds measured. These results are consistent with the rotor spacing with
460 maximum aerodynamic efficiency for this contra-rotating system, measured at $z/D = 0.3$ by
461 Chaitanya et al. (2020). Although the Aures/Terhardt tonality metric and More's and Di et al.'s
462 tonality factors suggest an optimal rotor spacing at $z/D \geq 0.35$, the psychoacoustic annoyance as
463 calculated with the three models implemented in this work significantly increases for rotor spacings
464 over $z/D = 0.4$. Furthermore, a rotor separation over $z/D = 0.4$ might be more impractical from a
465 construction perspective.

466 Below the optimal rotor spacing, the noise generation is dominated by potential field
467 interactions between the two contra-rotating rotors, which is consistent with previous observations
468 (McKay et al., 2019; Chaitanya et al., 2020). As the rotor spacing increases towards the optimum,
469 the magnitude of these potential field interactions lessens significantly, and therefore a decrease in
470 loudness is observed. As this source of noise is tonal in nature, tonality also drops significantly at the
471 optimum rotor spacing. This decrease in tonality, and especially loudness, lead to a minimum in
472 psychoacoustic annoyance. Fluctuation strength accounts for the slow amplitude modulation due to

closely spaced potential field interaction tones, and therefore drops importantly as the amplitude of these interaction tones decays.

With increased rotor separation distances after optimum, interaction noise between contra-rotating rotors increases due to enhance turbulence-propeller interactions, and this leads to an increase in loudness. Furthermore, as this is unsteady broadband noise in nature, roughness and impulsiveness increase when rotors move apart. This suggests that the perceptual effect of propeller-turbulence interaction noise could be accounted for by roughness and/or impulsiveness metrics.

A special case takes place when calculating sharpness as a function of rotor spacing. Sharpness reaches the highest values at the optimal rotor spacing region. As potential field interaction tones, distributed evenly along low-to-mid frequencies, decays significantly at the optimal rotor separation distance, the centroid of the spectrum moves towards the high frequency region (i.e. the relative contribution of high frequency tonal and broadband noise increases). Under these conditions of more dominant high frequency noise components, the values of sharpness are consequently higher.

The approach described in this paper, based on psychoacoustic methods available in the literature, provides a more sophisticated and comprehensive analysis than traditional sound power level analyses to inform the optimal design of rotating systems for lowest noise annoyance. Compared to sound power level based assessments, the proposed method is able to account for the key psychoacoustic features highly correlated to noise perception (e.g. tonality, roughness). Appropriately accounting for the perceptual effects of key psychoacoustic factors is crucial for the optimisation of designs for lower noise impact on potential exposed communities. As observed in this paper, minor deviations from the optimal design (in terms of rotor spacing) of contra-rotating propellers can lead to substantial increase in noise annoyance at emission angles typical for an observer on the ground interacting with a hovering UAV.

497 The three models implemented in this research gives the minimum psychoacoustic annoyance at
498 similar rotor spacings. Despite differences in tonality, these models are mainly driven by loudness.
499 Analysing findings of recent literature, the increase in the contribution (relative to loudness) of some
500 secondary factors (e.g. sharpness) required to become dominant for psychoacoustic annoyance
501 might be unrealistic. Based on the above, it could be argued that other psychoacoustic annoyance
502 models might also lead to the same conclusion in terms of optimum rotor spacing, and therefore,
503 the results of this paper are more general and no specific to the three annoyance models
504 implemented. However, this cannot be demonstrated without extensive testing, as it is uncertain
505 whether these psychoacoustic annoyance models provide an accurate picture of actual noise
506 perception for propeller noise (and specifically contra-rotating rotor noise). The relative
507 contribution to noise annoyance of different key psychoacoustic features in a variety of rotor noise
508 must be investigated to derive psychoacoustic annoyance models optimised for rotating systems.
509 Further work is recommended to aid the design of rotating systems for lowest noise impact: (1)
510 additional noise testing should be carried out to gather a comprehensive database with sound
511 samples of different blade geometries, thrust settings, emission angles and single vs. coaxial
512 propellers; (2) further analyses will include other psychoacoustic factors, such as impulsiveness,
513 relative approach and additional tonality models; and (3) extensive subjective testing should be
514 conducted to identify the psychoacoustic factors mainly driving rotor noise annoyance, refine or
515 compute coefficients accounting for their relative contribution to noise annoyance, and thus,
516 develop psychoacoustic annoyance models for rotor noise.

517 **ACKNOWLEGEMENTS**

518 The first author would like to acknowledge the financial support of the Royal Academy of
519 Engineering, United Kingdom (RF/201819/18/194). The authors would also like to thank Dr.
520 Mantas Brazinskas and Dr. Stephen Prior for their efforts in building this rig at the University of

Southampton. Dr Zhengguang Li would like to thank the funding of Natural Science Foundation of Zhejiang University of Science and Technology (No. 2019QN15).

REFERENCES

Aerospace Technology Institute (ATI) (2019). Accelerating Ambition: Technology Strategy 2019. Available at: https://www.ati.org.uk/media/siybi1mm/reduced-ati-tech-strategy.pdf (last accessed: 07/04/2020)

Alexander, W.N., Whelchel, J., Intaratep, N. and Trani, A. (2019). "Predicting community noise of sUAS." Proceedings of 25th AIAA/CEAS Aeroacoustics Conference, Delft, The Netherlands.

Angerer, R., Erickson, R.A., and McCurdy, D.A. (1991). "Development of an annoyance model based upon elementary auditory sensations for steady-state aircraft interior noise containing tonal components." NASA technical report TM 104147.

Anghinolfi, D., Canepa, E., Cattanei, A., and Paoluci, M. (2016). "Psychoacoustic optimization of the spacing of propellers, helicopter rotors, and axial fans." Journal of Propulsion and Power, 32(6), 1422-1432.

Aures, W. (1985a). "Ein Berechnungsverfahren der Rauhigkeit (A Calculation Method for Roughness)." Acustica 58, 268–280.

Aures, W. (1985b). "Berechnungsverfahren für den sensorischen wohlklang beliebiger schallsignale" ("A procedure for calculating sensory pleasantness of various sounds."). Acta Acustica united with Acustica, 59(2):130-141, 1985.

Barbot, B., Lavandier, C., Cheminee, P. (2008). "Perceptual representation of aircraft sounds." Applied Acoustics, 69, 1003-1016.

543 Berckmans, D., Janssens, K., Van der Auweraer, H., Sas, P., and Desmet, W. (2008). "Model-based
544 synthesis of aircraft noise to quantify human perception of sound quality and annoyance."
545 Journal of Sound and Vibration, 311, 1175-1195.
546 Boucher, M., Krishnamurthy, S., Christian, A., and Rizzi, S.A. 2020. "Sound quality metric indicators
547 of rotorcraft noise annoyance using multilevel regression analysis". Proc. Mtgs. Acoust. 36,
548 040004 (2019); doi: 10.1121/2.0001223
549 Brackley, M., and Pollock, C. (2000). "Analysis and reduction of acoustic noise from a brushless dc
550 drive." IEEE Transactions on Industry Applications, 36(3), 772-777.
551 Brazinskas, M. (2019). "An empirical investigation into interference effects of small-scale rotors for
552 use in vtol unmanned aircraft". PhD thesis, University of Southampton.
553 Cabell, R., Grosveld, F., and McSwain, R. (2016). "Measured noise from small unmanned aerial
554 vehicles." Proceedings of NOISE-CON 2016, Vol. 252, Institute of Noise Control
555 Engineering, Providence, RI, USA.
556 Chaitanya, P., Joseph, P., Prior, S. D., Parry, A. B. (2020). "On the optimum separation distance for
557 minimum noise of contra-rotating propellers." Journal of Fluid Mechanics (Under review).
558 The submitted version of the paper can be accessed upon request at:
559 http://eprints.soton.ac.uk/id/eprint/444759
560 Christian, A.W. and Cabell, R. (2017). "Initial investigation into the psychoacoustic properties of
561 small unmanned aerial system noise." Proceedings of the 23rd AIAA/CEAS Aeroacoustics
562 Conference, AIAA Aviation Forum, Denver, USA.
563 Daniel, P. (2008). "Psychoacoustical roughness." In Havelock, D., Kuwano, S., and Vorlander, M.
564 (Ed.). Handbook of signal processing in acoustics, Vol. 1, pp. 263-275. New York, USA:
565 Springer.

566 Di, G-Q., Chen, X-W., Song, K., Zhou, B., and Pei, C-M. (2016). "Improvement of Zwicker's
567 psychoacoustic annoyance model aiming at tonal noises." Applied Acoustics 105:164-170.
568 DIN 45631/A1-2010. "Calculation of loudness level and loudness from the sound spectrum -
569 Zwicker method - Amendment 1: Calculation of the loudness of time-variant sound."
570 DIN 45692-2009. "Measurement technique for the simulation of the auditory sensation of
571 sharpness."
572 Ercan, A. M. (2019). "Sound quality of small electric motors." Proceedings of InterNoise 2019,
573 Madrid, Spain.
574 Gwak, D.Y., Han, D., and Lee, S. (2020). "Sound quality factors influencing annoyance from
575 hovering UAV." Journal of Sound and Vibration, 115651.
576 HEAD Acoustics (2018). "Loudness and sharpness calculation." Technical Report Application Note
577 - 02/18
578 Heff, G.E. (1990). "Experimental performance and acoustic investigation of modern,
579 counterrotating blade concepts." NASA Contractor Report 185158.
580 Krishnamurthy, S.,Christian, A., and Rizzi, S. (2018). "Psychoacoustic test to determine sound
581 quality metric indicators of rotorcraft noise annoyance." Proceedings of Inter-Noise 2018
582 Impact of Noise Control Engineering, Chicago, USA.
583 Krishnamurthy, S., Rizzi, S.A., Boyd Jr., D.D., and Aumann, A.R. (2018). "Auralization of rotorcraft
584 periodic flyover noise from design predictions." Proceedings of the AHS International 74th
585 Annual Forum & Technology Display, May 14-17, 2018, Phoenix, Arizona, USA.
586 Lee, K.H., Davies, P., and Surprenant, A.M. (2005). "Tonal strength of harmonic complex tones in
587 machinery noise." Journal of the Acoustical Society of America 118, 1921.
588 Lee, J. (2016). "The effects of tones in noise on human annoyance and performance." PhD
589 dissertation, University of Nebraska.

590 Lee, J., and Wang, L.M. (2020). "Investigating multidimensional characteristics of noise signals with
591 tones from building mechanical systems and their effects on annoyance." Journal of the
592 Acoustical Society of America 147, 108-124.
593 Lyon, R.H. (2003). "Product sound quality – from perception to design." Sound and Vibration,
594 37(3), 18-23.
595 McMullen, A.L. (2014). "Assessment of noise metrics for application to rotorcraft." Master's Thesis,
596 Purdue University.
597 Magliozzi, B., Hanson, D.B., and Amiet, R.K. (1991). "Propeller and propfan noise." In Harvey H.
598 Hubbard, editor, Aeroacoustics of Flight Vehicles: Theory and Practice: Volume 1: Noise
599 Sources, number NASA RP-1258, pages 1–64.
600 Marte, J. E. & Kurtz, D. W. (1970). "A review of aerodynamic noise from propellers, rotors, and lift
601 fans." NASA Technical Report NASA-32-7462.
602 McKay, R.S., Kingan, M.J. and Go, R. 2019. "Experimental investigation of contra-rotating multi-
603 rotor UAV propeller noise." Proceedings of ACOUSTICS 2019, Cape Schanck, Victoria,
604 Australia.
605 Mestre, V., Fidell, S., Horonjeff, R.D., Schomer, P., Hastings, A., Tabachnick, B.G., and Schmitz,
606 F.A. (2017). "Assessing Community Annoyance of Helicopter Noise." Washington, DC:
607 The National Academies Press. Available at: https://doi.org/10.17226/24948.
608 More, S, and Davies, P. (2010). "Human Responses to the Tonalness of Aircraft Noise." Noise
609 Control Engineering Journal 58.4, 420–440.
610 More, S. (2011). "Aircraft noise metrics and characteristics." PhD Thesis, Purdue University.
611 Mosquera-Sánchez J.A., Villalba, J., Janssens, K., and de Oliveira, L.P.R. (2014). "A multi objective
612 sound quality optimization of electric motor noise in hybrid vehicles." Proceedings of

International Conference on Noise and Vibration Engineering (ISMA 2014), Leuven, Begium.

Perakis, G.J., Flindell, I.H., and Self, R.H. (2013). "Toward Roughness as an additional metric for aircraft noise containing multiple tones." Acta Acustica United with Acustica 99, 828-835.

Rizzi, S.A. (2016). "Toward reduced aircraft community noise impact via a perception-influenced design approach." Proceedings of InterNoise 2016, Hamburg, Germany.

Rizzi, SA., Burley, C.L., and Thomas, R.H. (2016). "Auralization of NASA N+2 Aircraft Concepts from System Noise Predictions." Proceedings of the 22nd AIAA/CEAS Aeroacoustics Conference. Lyon, France.

Sottek, R. (1993). "Modelle zur Signalverarbeitung im menschlichen Gehör" ("Models for signal processing in human hearing."). PhD thesis, RWTH Aachen.

Sottek, R., Vranken, P., and Busch, G. (1995). "A model for calculating impulsiveness" ("Ein Modell zrur Berechnung der Impulshaltigkeit"). Proceedings of DAGA 95 (German Acoustical Society Meeting), Saarbrücken, Germany.

Sottek, R., and Genuit, K. (2005). "Models of signal processing in human hearing". International Journal of Electronics and Communications (AEU) 59, 157-165.

Stract, W. C., Knip, G., Weisbrich, A. L., Godston, J. and Bradley, E. (1981). "Technology and Benefits of Aircraft Counter Rotation Propellers." NASA Technical Memorandum 82983. Available at: https://ntrs.nasa.gov/archive/nasa/casi.ntrs.nasa.gov/19830002859.pdf (last accessed: 07/04/2020)

Terhardt, E. (1974). "On the perception of periodic sound fluctuations (roughness)." Acustica 30, 548-560.

635 Terhardt, E., Stoll, G., and Seewann, M. (1982a). "Pitch of complex signals according to virtual-
636 pitch theory: Tests, examples, and predictions." Journal of the Acoustical Society of
637 America 71, 671-678.
638 Terhardt, E., Stoll, G., and Seewann, M. (1982b). "Algorithm for extraction of pitch and pitch
639 salience from complex tonal signals." Journal of the Acoustical Society of America 71, 679-
640 688.
641 Tinney, C.E. and Sirohi, J. (2018). "Multirotor drone noise at static thrust." AIAA Journal, 56(7),
642 2816-2826.
643 Torija, A.J., Roberts, S., Woodward, R., Flindell, I.H., McKenzie, A.R., and Self, R.H. (2019). "On
644 the assessment of subjective response to tonal content of contemporary aircraft noise."
645 Applied Acoustics, 146, 190-203.
646 Torija, A.J., Self, R.H., and Lawrence, J.L.T. (2019). "Psychoacoustic characterisation of a small
647 fixed-pitch quadcopter." In: Proceedings of InterNoise 2019, Madrid, Spain.
648 White, K., Bronkhorst, A.W., and Meeter, M. (2017). "Annoyance by transportation noise: the
649 effects of source identity and tonal components." Journal of the Acoustical Society of
650 America, 141, 3137-3144.
651 Zwicker, E. and Fastl, H. (1999). "Psychoacoustics – facts and models." Berlin: Springer-Verlag.